

Optical Properties of Injection-Molded Polystyrene Scintillators. I. Processing and Optical Properties

J. A. Martins,¹ J. Seixas,¹ J. Silva,^{2,3} V. Esteves,² M. J. Oliveira,¹ J. Gomes,² A. Maio,^{2,3}
A. S. Pouzada¹

¹Departamento de Engenharia de Polímeros, Instituto de Polímeros e Compósitos, Universidade do Minho, Azurém, 4800-058 Guimarães, Portugal

²Departamento de Física, Universidade de Lisboa, Campo Grande, Edifício C1, 1700-049 Lisboa, Portugal

³Laboratório de Investigação em Partículas, Av. Elias Garcia 14, 1000-149 Lisboa, Portugal

Received 17 April 2002; accepted 23 August 2002

ABSTRACT: Scintillating tiles for the Tilecal/Atlas calorimeter can be produced by injection molding, an alternative to mold casting via *in situ* polymerization. This new production method, which leads to a much faster production rate, introduces a number of additional variables that affect the optical yield of the scintillators and that have not yet been reported in the literature. In this work, the effect of processing-induced orientation on the optical properties of the scintillators is analyzed and discussed. For this purpose, the

birefringence across the thickness of the scintillator has been measured. The variations of the birefringence may be correlated with the orientation and, therefore, related to the optical performance, that is, the average light output and its nonuniformity. © 2003 Wiley Periodicals, Inc. *J Appl Polym Sci* 88: 2706–2713, 2003

Key words: fluorescence; injection molding; polystyrene

INTRODUCTION

Polystyrene (PS) scintillators produced by cast molding have been used since the early 1960s. These organic scintillators may be used as unitary systems composed of pure plastics (e.g., PS) or crystals, as binary systems of a plastic used as a solvent and a solute [e.g., *p*-terphenil (PTP)] used as a wavelength-shifting material, as ternary systems of a solvent and two solutes, or as even more complicated systems. A common feature of all organic scintillators is the presence of unsaturated aromatic molecules, which contain conjugated π -electron systems capable of fluorescing. The intrinsic quality of a scintillator may be characterized by its fluorescence and absorption spectra, the fluorescence quantum efficiency, and the fluorescence decay time.¹ Often, in practice, other related parameters are used for that purpose, such as the average light output, the nonuniformity, and the attenuation length.

Some of the first organic scintillators were made by the *in situ* polymerization of a PS solution with wavelength-shifting materials, that is, PTP and 2,2'-*p*-phenylene-bis(5-pheniloxazole) (POPOP). The solutes (PTP and POPOP) are commonly called primary and

secondary fluors because they act as fluorescent dyes. The radiation absorbed by the matrix is progressively shifted by the solutes from ultraviolet wavelengths to visible wavelengths and emitted.

For the production of large scintillators, this *in situ* polymerization process may take several days. In addition to the *in situ* polymerization, further steps are needed, such as heating for the completion of the polymerization, shock cooling for the release of the polymeric part from the reaction vessel, annealing, machining, and finishing.

In the 1950s and 1960s, these scintillators, in conjunction with fast photomultipliers, were used as scintillation counters with time resolutions below 1 ns. This made them suitable for studies of the lifetime of excited states of short-lived elementary particles (leptons, mesons, and hadrons).

In recent hadron calorimeters, such as the Tilecal/Atlas,² a very large number of scintillators have been needed. The Tilecal calorimeter is a subdetector of the Atlas multipurpose experiment for the Large Hadron Collider proton–proton collider. It is a cylindrical structure divided into 64 azimuthal modules. Each module consists of an assembly of steel plates (absorbers) and PS scintillators (active materials).

For the number of tiles needed for the Atlas tile calorimeter (ca. 460,000), injection molding is considered to be the most appropriate processing method because of its fast production rate and because it avoids the need for further thermal treatments and machining. This processing technique has been found

Correspondence to: J. A. Martins (jamartins@dep.uminho.pt).

Contract grant sponsor: Fundação para a Ciência e a Tecnologia; contract grant number: CERN/P/FAE/1191/98.

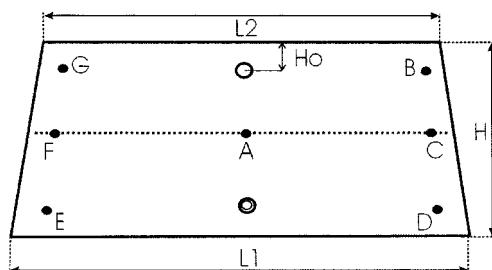


Figure 1 Dimensions of the scintillators ($L1 = 250$ mm, $L2 = 240$ mm, $H = 97$ mm, and $Ho = 13.5$ mm). The nominal thickness of the scintillators is 3 mm. It is desirable that the main dimensions be within a precision tolerance of ± 30 μm . The points used for the birefringence measurements with the wedge technique were, along the length, FAC; in the left-hand side to the gate, EFG; and in the right-hand side to the gate, DCB. The dashed line in the center shows the traveling line of the stimulation source.

to be adequate for this purpose at the Institute of High Energy Physics (Protvino, Russia).³ A comparison study was made between the optical properties of casting-molded and injection-molded scintillators, these having been processed with a cycle time of 1 min.⁴ In agreement with previous results,² the light yield in the injection-molded scintillators was 65–75% less than in cast scintillators. The sample dimensions were 3 mm \times 50 mm \times 90 mm. The measured attenuation length was about 40 cm and between 1.5 and 2 m for injection-molded and cast scintillators, respectively. Radiation hardness studies were also performed.

However, with injection molding, other variables are introduced, which affect the light output yield of the scintillators. These variables include the processing conditions (injection-molding temperature, injection rate, and mold temperature), the mold design and molding surface finishing, the orientation induced by processing, the raw material characteristics (molecular weight and molecular weight distribution, glass-transition temperature, and residual monomer content), and possible problems related to the additive distribution. The quality of these scintillators is assessed through the analysis of the light yield (absolute and relative), the average light yield uniformity, and the light attenuation length.

It was the purpose of this work to find a injection-molding solution to produce scintillators as free as possible from weld lines and not requiring postprocessing operations, to relate the processing conditions to the flow-induced orientation and the quality of the scintillators, to find a reliable and fast way of characterizing the raw material, and to link these data with the appropriate processing conditions. Also, it was considered important to evaluate the heterogeneity in the distribution of the dopants, their effective incorporation into the processed tiles, and their influence on the optical yield.

The adopted injection-molding solution and the processing conditions are discussed in the first part of the work. The measurement of the birefringence at different points of the scintillator is related to the orientation induced by the processing conditions. The analysis of the optical yield and nonuniformity can then be related to the processing conditions.

The relationship between the thermophysical properties and the processing conditions, as well as an evaluation of the role of a heterogeneous distribution of dopants, is presented in the second part of this work.

EXPERIMENTAL

The Tilecal/Atlas calorimeter makes use of 11 different sizes of trapezoidal scintillators.^{2,5}

Scintillators

The scintillator chosen for this study was of a size moldable in the small injection-molding machine with a 600 kN clamping force available at the University of Minho. The main dimensions of the scintillator used in this study are shown in Figure 1.

Molding solution

Previous mold solutions for the production of the Tilecal scintillators involved the use of one or more film gates located at the central zone of the longer edge ($L1$). These solutions have, as major disadvantages, the formation of a long weld line between the two holes in the center of the molding and the requirement of a postprocessing machining operation for a smooth surface to be obtained at the edge at which the gating is made. The solution developed at the University of Minho, as a major feature, shows a diaphragm gate located at the hole closer to $L1$, as shown in Figure 2.

This solution allows for a nearly weldless molding requiring no relevant finishing operations. The removal of the sprue, without damage to the scintillator surface, can be easily accomplished by the operator, who performs a quick reaming of the hole while the next molding is in progress. The analysis

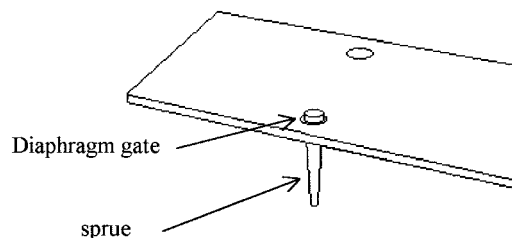


Figure 2 Diaphragm gate solution for the scintillators.

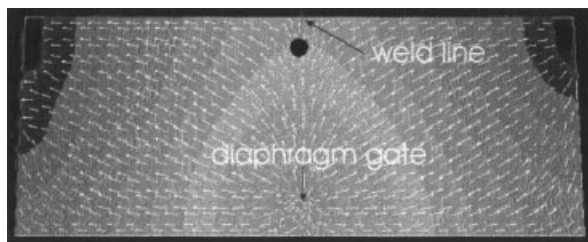


Figure 3 Moldflow simulation of the temperature distribution in the scintillators (tile 65). The different gray areas correspond to different temperatures. The difference between the lighter (hotter) and darker (cooler) areas is 3°C. The weld line is indicated.

of the flow in this molding was done with the Moldflow simulation program (Moldflow Pty, Victoria, Australia). In these analyses, the possibility was explored of obtaining temperature and shear stress fields as uniform as possible. In fact, the shear stress is determinant for the buildup of the molecular orientation, and the temperature uniformity leads to a lesser anisotropy of the molding properties (optical), as it is required in this product. In Figure 3, for typical molding conditions, the great uniformity of the temperature field is evident. Figure 3 also shows the flow lines during filling; the weld line is created at a noncritical zone, between the hole and the edge, which are farther from the diaphragm gate. This solution was implemented in the prototype mold for this study and is recommended for the mass production of scintillators for tile calorimeters.

Molding conditions

The scintillators were produced in a molding cell consisting of a Krauss Maffei 61 210A injection-molding machine (Munich, Germany) with a 600 kN clamping force and a thermoregulator for control over the mold temperature. Typical processing conditions are shown in Table I.

In addition to these conditions, different settings were also used for the assessment of the influence of processing. In particular, the mold temperature, which was coupled to the freezing off of the molecular orientation in the parts, was varied between 30 and 80°C

TABLE I
Typical Injection-Molding Conditions

Parameter	Value
Injection pressure (MPa)	16
Holding pressure (MPa)	8
Back-pressure (MPa)	1
Holding time (s)	5
Cooling time (s)	45
Temperature profile (°C)	220–200–196
Mold temperature (°C)	40

TABLE II
MFR, Molecular Mass, and Glass-Transition Temperature (T_g) of PS

Manufacturer	Grade	MFR (g/10 min)	Molecular mass (g/mol)	T_g (°C)
	Polystyrol, 143E	10	6,000	84.1
BASF	Polystyrol, 158K	3	380,000	102.4
Monsanto	Edistir N 1840	10	10,000	86.91
PSM	115	13.4	20,000	96.5

in steps of 10°C. The injection temperature of 220°C was kept throughout the experiment.

The switching between the injection and holding phases in the injection cycle was made as a function of the maximum injection pressure. Nevertheless, the mold was designed and prepared to work with a pressure sensor in the mold cavity to more accurately control this critical switching phase. The moldings, which were removed manually from the mold to prevent damage from falling, were produced at intervals of 2 min to guarantee the reproducibility of the characteristics. The long cooling time in the mold was sought to allow a slow cooling of the molding, which led to a smaller level of residual thermal stresses and minimal warpage. All the moldings were weighed after molding for continuous tracking of the repeatability of the process.

Materials

PS

A number of commercial grades of PS, suitable for optical applications, were used in this study. Some were produced as standard grades by EU companies. One grade of AKPO, Kazakhstan (PSM 115) was also used, as it was the material used in the preliminary studies and quoted for the light yield performance of the scintillators. Nevertheless, it is unlikely that this grade will be used in mass production because of difficulties at the polymerization plant.

The materials were characterized in terms of the melt-flow rate (MFR) and the major properties, as shown in Table II. The values of the glass-transition temperature were obtained according to an experimental procedure that is discussed in the second part of this work and was also used in the evaluation of the molecular mass values (which are shown in the same table).

The data for the glass-transition temperatures and estimated molecular masses for Polystyrol 143E and Edistir N 1840 appear to be not compatible with the MFR data, especially when the PSM 115 data are considered. A clear reason for this discrepancy is not clear, but the fact that the Polystyrol and Edistir materials have optical properties inferior to those of PSM

TABLE III
Dopant Properties

	PTP C ₁₈ H ₁₄	POPOP C ₂₄ H ₁₆ N ₂ O ₂
M_r (g)	364.41	230.31
λ_{\max} (nm)	358	277
T_m (°C)	243–246	212–213
Log ϵ	4.72	4.50

M_r = molecular mass; λ_{\max} = maximum absorption wavelength; T_m = melting temperature; ϵ = coefficient of molar extinction.

suggests that the additive systems used during the polymerization are substantially different. Nevertheless, in this work, there was no possibility of investigating further this peculiar aspect.

Dopants

Two dopants from Fluka (Buchs SG, Switzerland) were used for promoting the fluorescence of the scintillators: PTP and POPOP. Their main properties are listed in Table III.

Mixing

The mixing of the dopants with PS was done in a tumble mixer at room temperature for 1 h. The mixture was done in batches of 50 kg. The composition by weight was that considered optimal in the Atlas Technical Proposal:¹ 98.45% PS, 1.5% PTP, and 0.05% POPOP.

Production

Before processing, the material was predried in an oven at 70°C. For each set of processing conditions and materials, at least 50 moldings were produced in process-stabilized conditions. The moldings were individually controlled in weight after the molding and the removal of the sprue. The average weight was calculated, and the scintillators differing from this value more by than one standard deviation were discarded for further testing.

Also, the shrinkage of the moldings, processed under the same processing conditions, was calculated on a batch of 50 moldings, 2 and 10 days after the molding. Table IV shows the average results obtained for the two grades of Polystyrol. The precision of this data is in agreement with the specifications concerning the dimensional accuracy of the moldings.

Optical properties

The optical properties were assessed in terms of the light output of the stimulated scintillator and the

molding birefringence. The optical properties of the scintillators were measured with X-rays and a stabilized ultraviolet light source⁶ after the positioning of the stimulation source at different positions on the surfaces of the scintillators.

The stimulation was made by a ⁹⁰Sr β source, placed on an XY table. The position of the source was controlled by a computer. Upon stimulation, the scintillator produced light that was collected by wavelength-shifting optical fibers, which were located at opposite sides of the tile and with a configuration similar to that of the Tilecal Atlas calorimeter. The light was then transmitted to photomultiplier tubes (PMTs), which converted the light signal into electric pulses that were read and recorded. The two PMTs (PMT1 and PMT2) were located on opposite sides of the tile. A computer program allowed the simultaneous control of the ⁹⁰Sr β source position and the storage of the readouts alongside the corresponding source coordinates. This program enabled us to assess the tile optical performance in several different modes: the readout of a single point, linear scanning, and two-dimensional scanning. For optical characterization, the linear scanning mode in the X direction is commonly used to make a pass over the central region of the scintillator.

The measurement of the birefringence was made by the wedge technique⁷ with triangles with dimensions of approximately 25 mm \times 14.4 mm \times 29.9 mm and defining angles of 30, 60, and 90°. These triangles were cut from selected parts of the scintillators at three points near the edges and close to the diaphragm gate. The selected points are shown in Figure 1: along the length of the scintillator (points F, A, and C) and along the width in the left-hand side to the gate (points E, F, and G) and in the right-hand side to the gate (points B, C, and D).

The edges of the triangles were polished with grinding paper, which started with a roughness of 320 and ended at 4000. The polished triangles were mounted in a handler, with the tip of the edge with the minor angle facing up. The handler was then immersed in paraffin oil and viewed in an optical microscope between crossed polars with a quasimonochromatic light source ($\lambda = 550$ nm). For a reduction in the number of errors, the value of the minor angle of the triangle was measured in a low-magnification microscope. The measurements of the bire-

TABLE IV
Shrinkage of Moldings Processed Under the Same Conditions Measured 2 and 10 Days After Processing

Grade	2 days (%)	10 days (%)
Polystyrol 143E	0.512	0.524
Polystyrol 158K	0.558	0.572

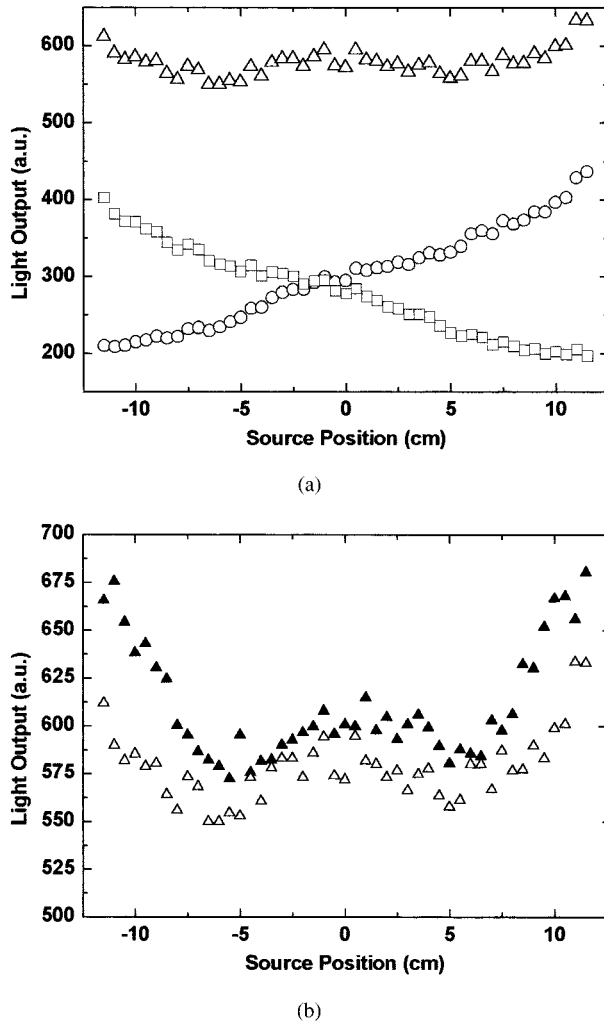


Figure 4 (a) Light output chart of tile 136 (central scan): (○) PMT1 readout, (□) PMT2 readout, and (△) total readout. (b) Nonuniformity evaluated through measurements of the light output for (▲) tile 16 and (△) tile 136.

fringe were taken at five different points along the sample thickness for samples collected along the width and length of the scintillators with specific optical characteristics.

The birefringence was calculated as follows:

$$\Delta n = \frac{\lambda}{l \cdot \tan \alpha} \quad (1)$$

where l is the spacing between two extinction bands and α is the angle at the edge of the triangular sample, which is nearly 30° . The accuracy of the measurements for each sample were improved with a magnified digital image of the observation.

RESULTS AND DISCUSSION

Light output

A typical plot of the light output measurements for a scintillator is shown in Figure 4(a). From a typical scan like this one, information on the average light output and nonuniformity of the tile response can readily be obtained. The average light output is the mean value of the sum of the individual readouts from the PMT. The nonuniformity is evaluated from the ratio between the standard deviation of the total readout (PMT1 and PMT2) and the average light output. One of the design specifications for the Tilecal requires that the nonuniformity should not exceed a 5% rms (root mean square) for all the tiles.

From each PMT readout, a rough estimate of the attenuation length of the tile can be obtained. The procedure consists of dividing the individual PMT readout curve into smaller sections that show an approximately exponential behavior. From the fitting parameters, the estimated value is obtained. Acceptable values for the attenuation length should be around 300 mm or higher.

The values obtained for a small but representative set of scintillators are shown in Table V. The corresponding processing conditions are presented in Table VI. Because of the differences in the optical properties, evaluated through the average light output and average attenuation length (Table V), and in the processing conditions (Table VI), we selected tiles 16 and 136 to illustrate the effect of the processing conditions on the optical properties. Comparing the data shown in Figure 4(b) for the light output of two different scintillators (numbered as 16 and 136) produced under different processing conditions, we find that tile 16 displays a slightly higher light output but shows a worse nonuniformity than tile 136.

The optical performance of the tiles depends not only on the average output but also on the nonuniformity

TABLE V
Average Light Output and Attenuation Length for Selected Scintillators

Tile	Material	Injection temperature ($^\circ\text{C}$)	Average light output (au)	Average attenuation length (mm)
16	BASF 158 K	185	610	250
17	BASF 158 K	185	612	258
136	BASF 158 K	175	578	299
173	PSM 115	175	593	289
178	PSM 115	200	623	330

TABLE VI
Processing Conditions of the Scintillators in Table V

Tile	Material	Injection pressure (MPa)	Hold-on pressure (MPa)	Back-Pressure (MPa)	Temperature profile (°C)
16	BASF 158K	14	14	2	185/185/180/180/175
17	BASF 158 K	14	14	2	185/185/180/180/175
136	BASF 158 K	15	15	3	175/175/175/165/165
173	PSM 115	12	12	3	175/175/175/165/165
178	PSM 115	19	19	1.5	200/195/190/185/180

Mold temperature = 60°C.

mity and average attenuation length. The data presented in Table V show that tiles 16 and 17 (which belong to the same set) do not conform to the specified requirements.

Concerning the optical characteristics of the tiles produced with BASF and PSM PS, what comes out of our results is that the average light output of the tiles is very close for every tile, being separated by less than 10% for the extreme values. It was not possible to get a clear indication of what material would have the highest light output, but the values that were obtained showed that an increase of 10% or higher in the light output relative to the tiles produced in Protvino for the 1996 prototype Module 0 could be reached, for both materials, as long as the processing conditions were optimized.

For the average attenuation length, we obtained consistently increased values, with respect to the Module 0 reference, of up to 30% for PSM 115. The majority of the BASF tiles produced (similar to tiles 16 and 17) had a slightly inferior attenuation length with respect to the reference, except for those of a batch bought in Russia (including tile 136), for which increases of up to 23% were observed.

Those tiles, which were processed with different injection temperatures and pressure conditions, necessarily had different levels of flow-induced orientation, which was reflected in the optical properties. As stated previously, the orientation was assessed by the measurement of the birefringence at different points along the thickness and specific sample positions. The results are analyzed in the next section.

Birefringence and optical performance

In injection moldings, the flow-induced orientation of the polymer molecules and the frozen-in stresses, because of the nonuniform rate of cooling, are frequent sources of anisotropy. The birefringence is an optical property widely used for quantifying the level of the optical anisotropy of transparent articles.

The data in Figure 5(a,b), in which the birefringence variation across the thickness and along the length is plotted, illustrate well the role of the flow-induced orientation in this property. As expected, the birefrin-

gence is at a minimum at the half-thickness of the tile for which the shear stress during injection and the cooling rate are at a minimum. The birefringence increases toward the sample surface, accompanying the rise of the shear stress and the cooling rate, which

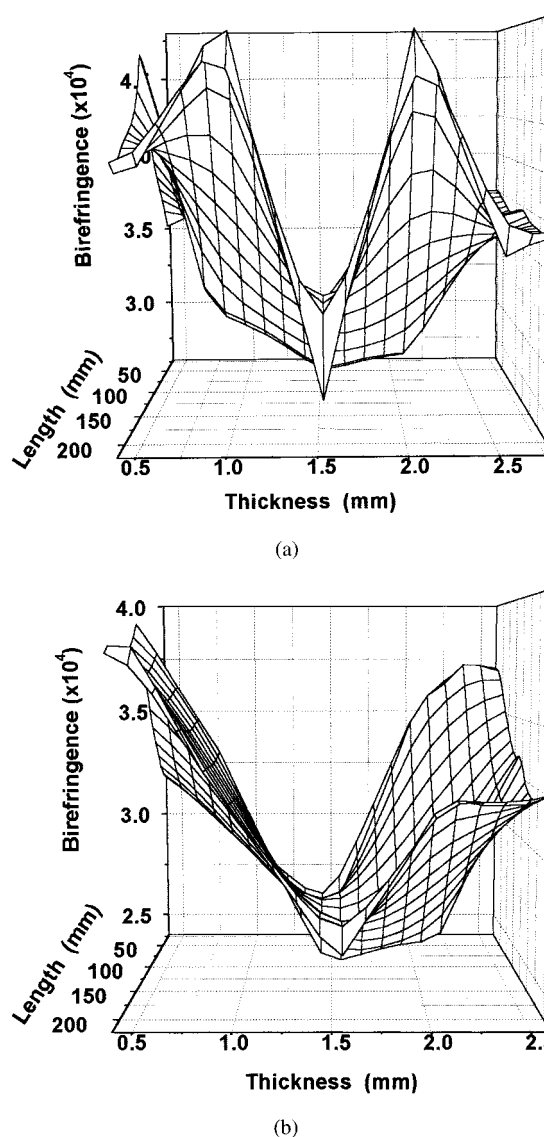


Figure 5 Variation of the birefringence along the length and width for (a) tile 16 and (b) tile 136.

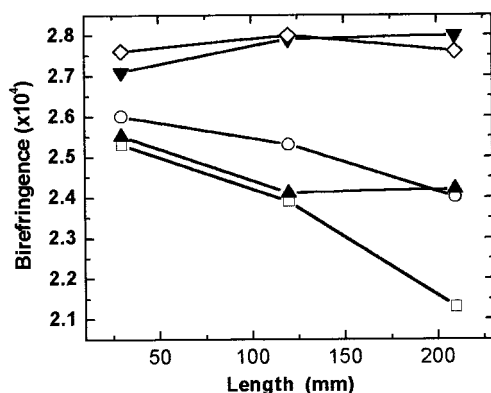


Figure 6 Variation of the birefringence along the length of the scintillator for the tiles indicated: (▲) tile 136, (▼) tile 16, (○) tile 173, (□) tile 178, and (◇) tile 17. The measurements were taken at positions F, A, and C, which corresponded to points at 30, 120, and 210 mm, respectively.

favor the freezing-in of the molecular orientation in the molding. These figures also illustrate the complexity of the pattern of the variation of the birefringence across the thickness and through the length of the tiles. For simplicity, only the values of the birefringence at approximately half of the tile thickness (between 1.47 and 1.53 mm) are analyzed in relation to the molding conditions and light output.

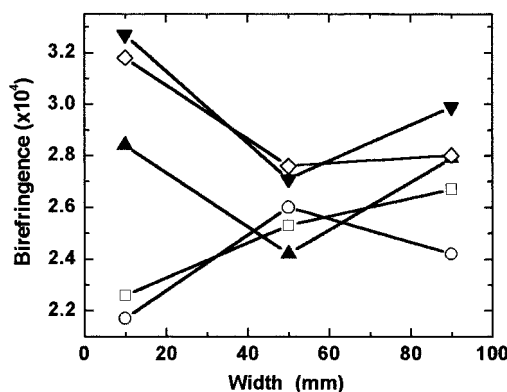
The variation of the middle plane birefringence along the length of the tiles is shown in Figure 6 for specimens made from the two types of raw materials under different molding conditions. As expected, the values of the birefringence of tiles 16 and 17 are very close. As these specimens were produced with the same material and under the same processing conditions, the observed differences resulted from the inevitable variations inherent in the molding process, the sample preparation, and the experimental errors associated with the birefringence measurement method.⁸

The plots of Figure 6 show that the birefringence is affected in a complex manner by factors related to the material and the processing conditions. A comparison of the birefringence results for tiles 16 and 17 with those of tile 173 confirms that the molecular weight of the material has a great influence on the setting up of the molecular orientation in the moldings, which increases with the molecular weight. Tile 173, despite being molded with a lower melt temperature than that used for tiles 16 and 17, presents lower birefringence than the latter, and this can only be explained by the lower molecular weight (higher MFR) of the material used in tile 173. This argument may also be used to explain the differences in the behavior shown by tiles 173 and 178.

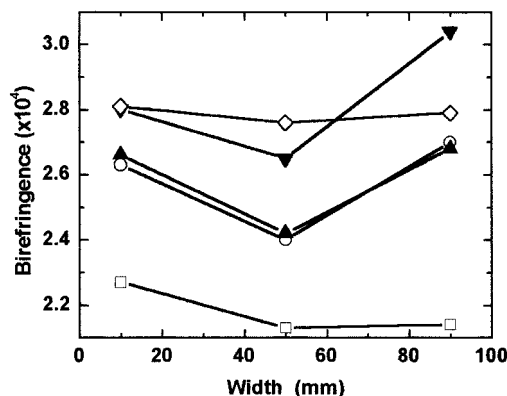
Although it is difficult to establish a trend of variation resulting from varying processing conditions for tiles of the same material, tiles 173 and 178, both from PSM 115, do show a smaller birefringence, even though the comparative variation is small.

The analysis of the symmetry of birefringence was evaluated through the measurements of the birefringence along the width of the scintillators, at the left-hand and right-hand sides to the gate, as shown in Figures 7(a) (positions E, F, and G in Fig. 1) and 7(b) (positions B, C, and D in Fig. 1), respectively. Although the experimental error may be relevant, as suggested by the results for tiles 16 and 17, the difference in the birefringence between the left and right sides of the tiles shows that the symmetry is not perfect.

A consistent trend is found when the results of Figures 6 and 7 are compared against those of Figures 4 and Table V. The scintillators with higher values for the birefringence have poor optical properties (worse nonuniformity and lower attenuation length). Although for the cast-molded scintillators the orientation is an irrelevant parameter, the molecular orientation in injection-molded scintillators seems to play an important role in their optical performance. Therefore, reduced anisotropy seems to favor the optical yield.



(a)



(b)

Figure 7 Variation of the birefringence along the width for samples collected (a) in the left-hand side to the gate at positions G, F and E, which corresponded to points at 1 cm, 5 mm, and 9 cm, respectively, and (b) in the right-hand side to the gate at positions B, C, and D, which corresponded to the same points: (▲) tile 136, (▼) tile 16, (○) tile 173, (□) tile 178, and (◇) tile 17.

Another factor that may affect the optical yield and nonuniformity of the scintillators is the distribution of the dopants. The back-pressure, acting during the plasticization of the material for injection, has a major effect on the homogenization of the melt, especially when additives are used. As shown in the second part of this work, the lower back-pressure used in the processing of tiles 16 and 17 is responsible for an inhomogeneous distribution of the dopants within the PS matrix, and this may also contribute to the poor optical performance of these tiles.

The molecular weight of the raw material is a parameter that can be handled by the tuning of the processing conditions, that is, the back-pressure, because materials with lower molecular weights do not need to be highly back-pressurized for a homogeneous distribution of dopants to be obtained.

For improved optical performance, tiles with good and bad optical yields were annealed at temperatures between 50 and 90°C. A general decrease was found for the optical yield for all the tiles, the average light output being hardly measurable. The explanation for these results requires the consideration of two anisotropic effects: one due to the orientation induced by processing, which affects the optical yield in a manner previously described, and the other due to the anisotropy in the distribution of the solutes (wavelength shifters) in the scintillator. This distribution is important, and it is analyzed in detail in the second part of this work.

A possible explanation for the observed results in the annealed scintillators is that, although the anisotropy caused by orientation is relaxed, another anisotropic effect appears. In fact, by favoring the rearrangement of the polymer chains to more entropic states, the annealing also induces the movement of the primary and secondary solutes, thereby contributing to an increase in the anisotropy in the solute distribution. The solutes may then be distributed more heterogeneously in the tiles, both along the length and along the thickness, thereby contributing to a decrease in the optical yield.

Another parameter that is known to affect the optical properties of scintillators, at least in cast scintillators,¹ is the residual monomer content. This parameter was not assessed in the project materials used in this work, but according to the information already gathered in the Tilecal Atlas project, it must always be less than 0.1%.²

The fluctuations in the optical properties of the scintillators resulting from the injection molding are a topic recognized in the Atlas Technical Report as needing further development.² The data in this work suggest that fluctuations of the scintillator optical

properties depend on the raw material optical properties and on the appropriate choice of the processing conditions. The stability of the injection-molding process and the mold filling are also important, but in this work, these requirements have been achieved, as illustrated by the small variation of the optical properties (the attenuation length and birefringence) shown by tiles 16 and 17, which were processed under the same conditions.

CONCLUSIONS

A molding solution with a fast production rate has been developed for producing scintillators for the Tilecal Atlas calorimeter, based on the injection molding of doped PS. The developed solution reduces the post-processing operations and improves the homogeneity and regularity of the moldings.

The data from tiles produced with several raw materials and under different processing conditions enabled us to establish a correlation between the processing-induced orientation and the final optical performance, that is, the optical yield and nonuniformity.

It has been concluded that a lower birefringence is related to a higher optical yield, which is also dependent on a stable (and approximately constant) birefringence along the length of the scintillator.

The processing conditions in the production of the scintillators must be adjusted to improve the homogenization of the melt: this objective is achieved through control over the back-pressure during the plasticization of the melt.

Special thanks are due to P. Peixoto of the Department of Polymer Engineering at the University of Minho for assistance with the mold design.

References

1. Birks, J. B. *The Theory and Practice of Scintillation Counting*; Pergamon: New York, 1964.
2. Atlas Tile Calorimeter; Technical Design Report CERN/LHC/96-42, Atlas TDR 3; CERN: Geneva, Switzerland, 1996.
3. Karyukhin, A.; Kopikov, S.; Kostrikov, M.; Lapin, V.; Zaitsev, A. Injection Molding Scintillator for Atlas Tile Calorimeter; Atlas Internal Note Tilecal-96-086; CERN: Geneva, Switzerland, 1996.
4. Yoshimura, Y.; Inagaki, T.; Moromoto, T.; Sugai, I.; Kuriki, M.; Shirai, R.; Goto, M.; Yamashina, T. *Nucl Instrum Methods Phys Res Sect A* 1998, 406, 435.
5. Cobal, M.; Lapin, V.; Nessi, M.; Shoultz, D. Measurement of Some Optical Properties of the Tiles for Module 0; Atlas Internal Note CAL-NQ-81; CERN: Geneva, Switzerland, 1996.
6. Amaral, P. Graduation Thesis, University of Lisbon, 1995.
7. Hemsley, D. A.; Robinson, A. M. *Polym Testing* 1992, 11, 373.
8. Neves, N. M.; Pouzada, A. S.; Voerman, J. H. D.; Powell, P. C. *Polym Eng Sci* 1998, 38, 10.